

Solvatochromism and the effect of solvent on properties in a two-dimensional coordination polymer of cobalt-trimesate

Savannah C. Zacharias,^{a†} Gaëlle Ramon,^a Susan A. Bourne^a

^aCentre for Supramolecular Chemistry Research, Department of Chemistry, University of Cape Town, Rondebosch, Cape Town, 7701, South Africa. *Correspondence e-mail: susan.bourne@uct.ac.za

†Present address

University of Gothenburg, Department of Chemistry and Molecular Biology, Kemivägen 10, SE-412 96, Gothenburg, Sweden.

Supporting Information

Crystallography

$[\text{Co}(\text{btc})(\text{DMF})_2] \cdot x \text{DMF}]_n$ (**1**)

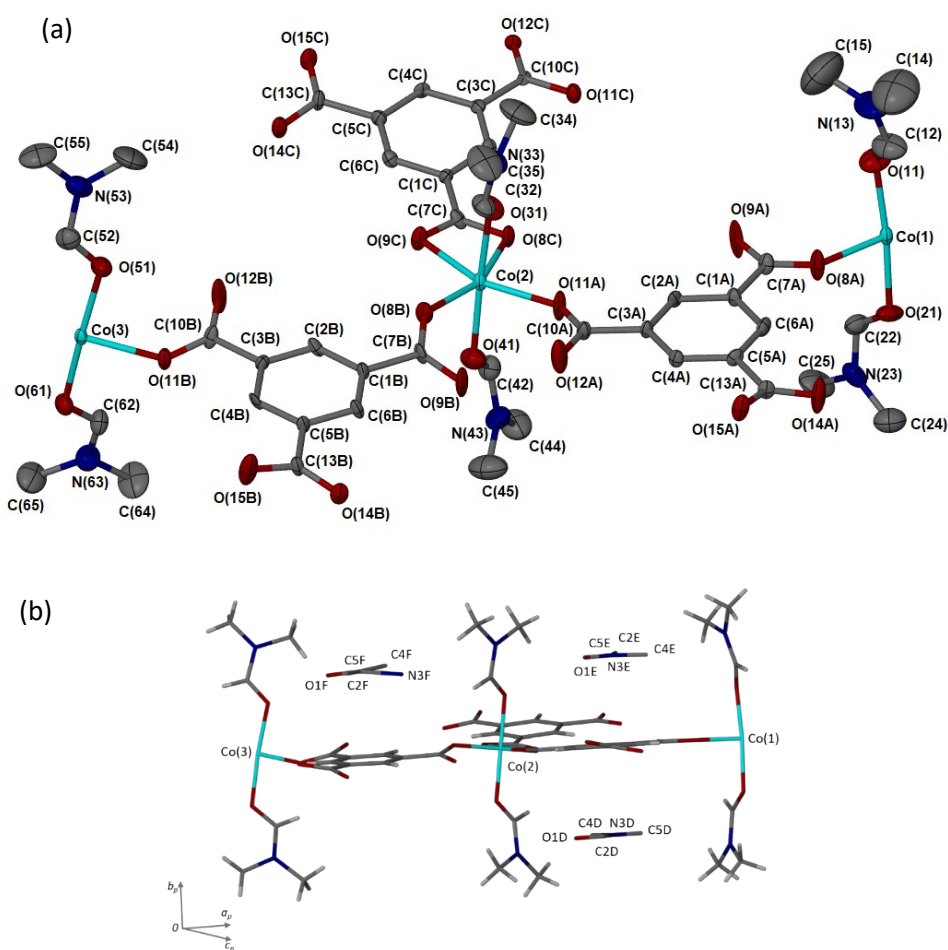


Fig. S1. Asymmetric unit of **1** showing ADP's at 50% probability, with hydrogen omitted for clarity. b) The positioning of the DMF solvent molecules within the asymmetric unit.

Table S1. Coordination geometry of the ligands to the metal centres of **1**

Bond	Distance [Å]	Bond	Angle [°]
Co1—O8A	2.053(5)	O8A—Co1—O11	87.5(2)
Co1—O11	2.075(6)	O8A—Co1—O21	88.7(2)
Co1—O21	2.109(6)	O11—Co1—O21	175.0(2)
Co2—O8B	2.056(5)	O11A—Co2—O8C	94.2(2)
Co2—O8C	2.153(5)	O8B—Co2—O11A	107.9(2)
Co2—O9C	2.140(5)	O9C—Co2—O8C	61.4(2)
Co2—O11A	2.054(5)	O8B—Co2—O9C	96.4(2)
Co2—O31	2.124(6)	O31—Co2—O41	175.6(2)
Co2—O41	2.106(6)		
Co3—O61	2.129(4)	O11B—Co3—O51	88.1(2)
Co3—O51	2.055(6)	O11B—Co3—O61	90.1(2)
Co3—O11B	2.054(5)	O51—Co3—O61	174.1(2)

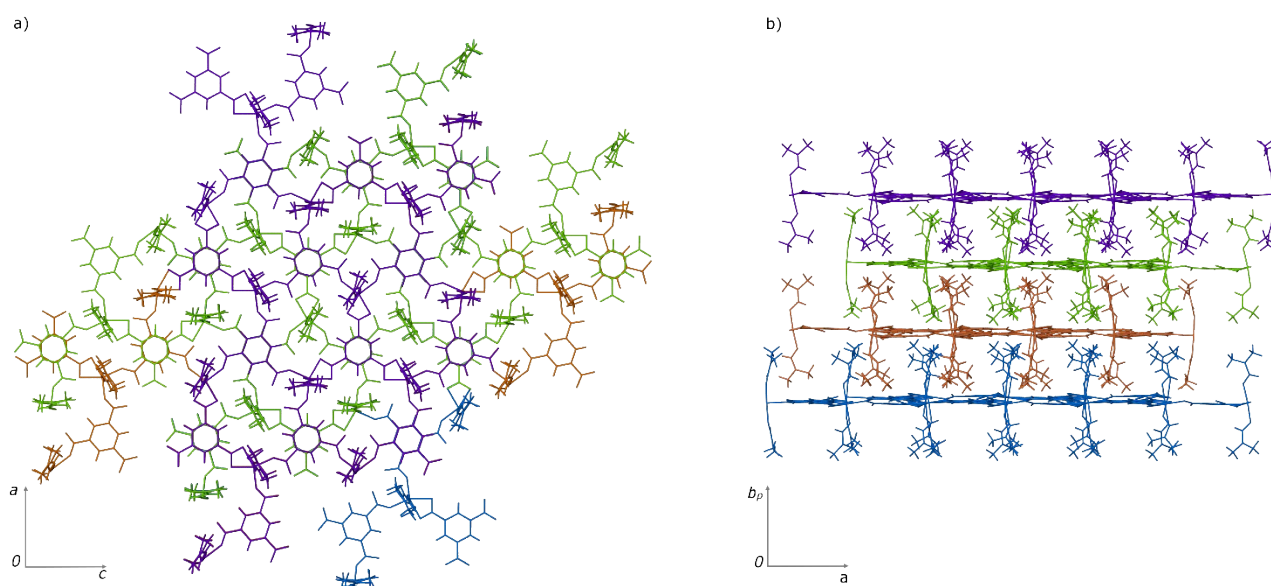


Fig. S2. Packing of **1**, viewed down a) [010] and b) [001]. The interdigitated layers propagate along [100] and [001]. The unbound DMF solvent has been omitted for clarity.

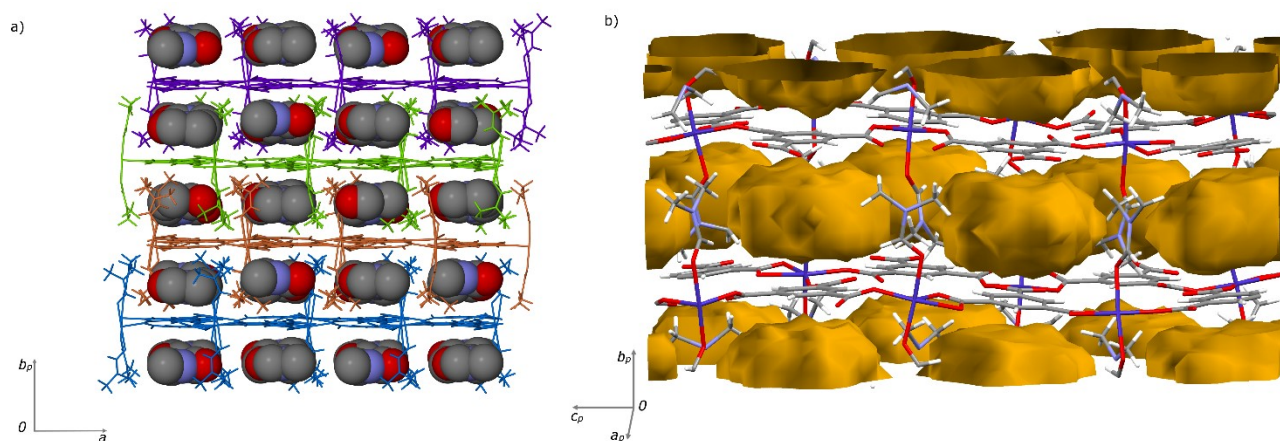


Fig. S3. Packing of **1** a) The DMF solvent molecules, in space-fill display, are in the channels formed between layers along the $[001]$ axis. b) Calculated cavities which stack one above the other parallel to $[010]$ and form a zig-zag pattern parallel to $[001]$.

Hydrogen bonding in **1**

Table S3. Summary of hydrogen bond lengths and angles for **1**

Number	Hydrogen bond	D—H*	H \cdots A*	D \cdots A	D—H \cdots A*	Symmetry
		[Å]	[Å]	[Å]	[°]	Operation
1	C22—H22 \cdots O14B	0.95	2.47	3.028(11)	117	1+x, y, z
2	C32—H32 \cdots O8B	0.95	2.48	3.057(11)	119	
3	C42—H42 \cdots O8C	0.95	2.57	3.202(11)	124	
4	C52—H52 \cdots O12C	0.95	2.60	3.186(11)	120	-1+x, y, z
5	C62—H62 \cdots O11B	0.95	2.50	3.067(10)	119	
6	C55—H55C \cdots O1D	0.98	2.55	3.52(2)	168	1/2-x, 1/2+y, 1/2-z
7	C24—H24B \cdots O14A	0.98	2.59	3.510(15)	157	2-x, 1-y, 1-z
8	C24—H24C \cdots O14C	0.98	2.52	3.411(14)	151	3/2-x, -1/2+y, 1/2-z
9	C25—H25A \cdots O9C	0.98	2.50	3.291(15)	137	3/2-x, -1/2+y, 1/2-z
10	C25—H25B \cdots O12B	0.98	2.59	3.555(16)	167	3/2-x, -1/2+y, 1/2-z
11	C35—H35C \cdots O11C	0.98	2.56	3.396(15)	144	3/2-x, 1/2+y, 1/2-z
12	C44—H44C \cdots O8C	0.98	2.57	3.369(14)	139	3/2-x, -1/2+y, 1/2-z
13	C45—H45B \cdots O11C	0.98	2.57	3.412(15)	144	3/2-x, -1/2+y, 1/2-z
14	C64—H64B \cdots O15C	0.98	2.48	3.350(14)	147	1-x, 1-y, -z
15	C64—H64C \cdots O9B	0.98	2.58	3.547(15)	170	1/2-x, -1/2+y, 1/2-z

*e.s.d values not calculated as hydrogen atoms were placed in geometrically idealised positions.

PXRD

Fig. S4 shows the PXRD patterns of the calculated and experimental of **1** as well as the starting materials. The experimental pattern is not a sum of the patterns of the starting materials, indicating a new phase has been formed. The reasonable agreement between the calculated and experimentally obtained patterns shows the homogeneity of the bulk material.

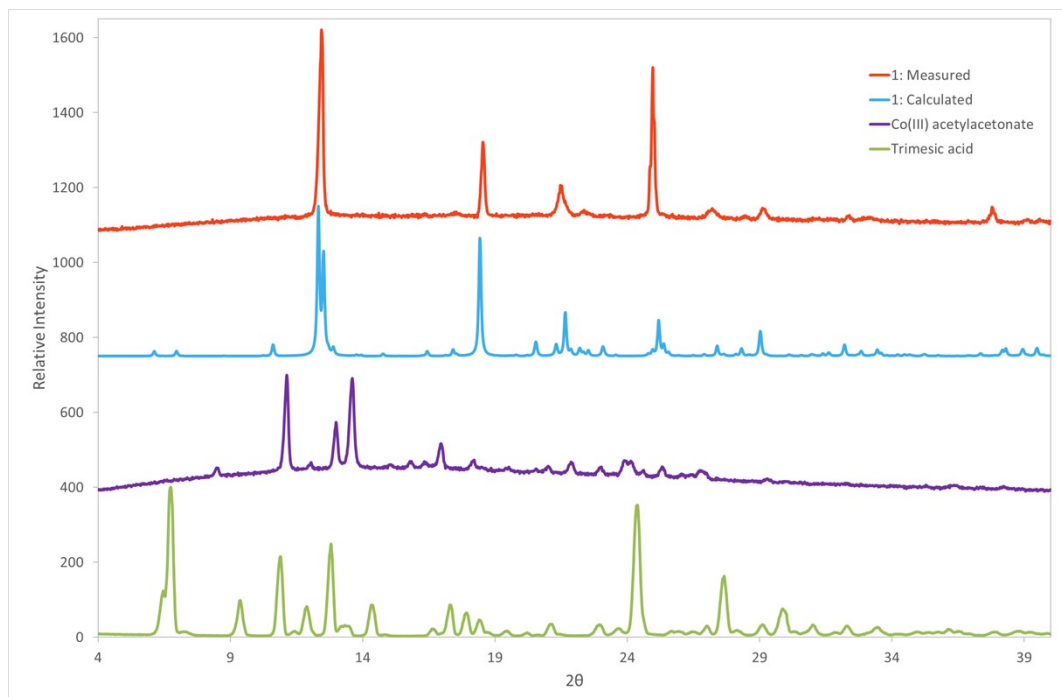


Fig. S4. PXRD patterns of cobalt(III) acetyl acetate, trimesic acid and the calculated and experimental patterns of **1**. A new phase is present.

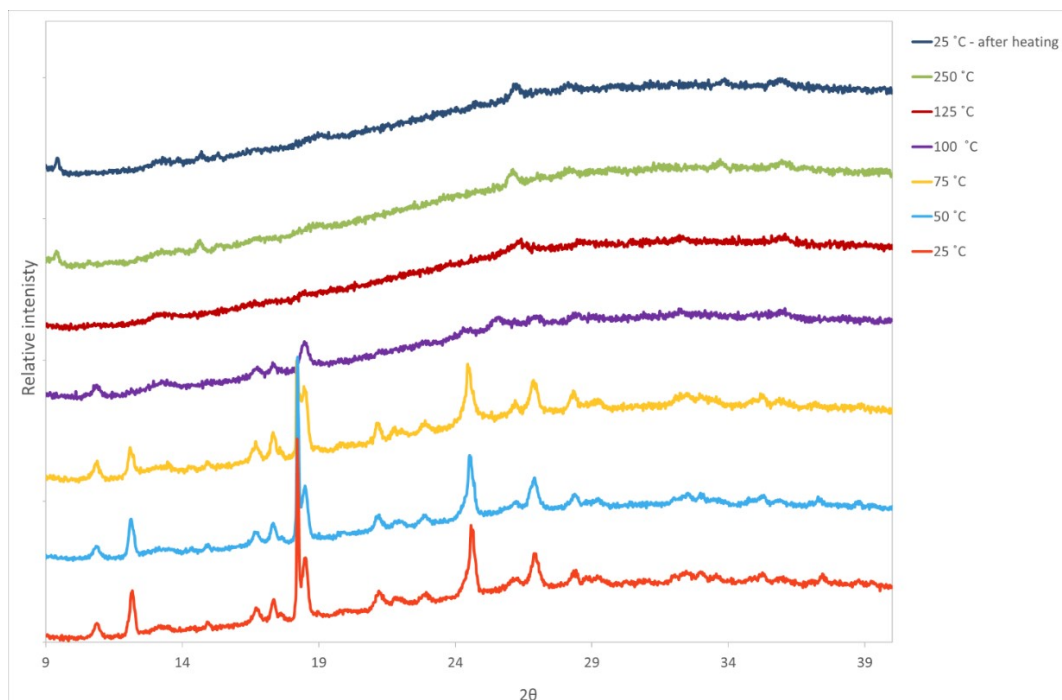


Fig. S5. Variable temperature PXRD patterns of **1** from 25 °C to 125 °C, after which the pattern is unchanged. Crystallinity is lost at ca. 75 -100 °C as the DMF guests have been removed.

Thermal Analysis

The eight DMF molecules in the crystal structure are removed in three successive steps as seen in the TGA trace (Fig. S6). This three-step mass loss of $40.8 \pm 0.8\%$ occurs between $88.6 \pm 2.7\text{ }^\circ\text{C}$ and $248.0 \pm 0.6\text{ }^\circ\text{C}$ ($n = 3$). The first step is most likely the loss of DMF in the channels, followed by the loss of the coordinated DMF molecules as more energy is required to remove them. The subsequent loss of $31.4 \pm 0.3\%$ between $343.81 \pm 2.2\text{ }^\circ\text{C}$ and $495.1 \pm 0.7\text{ }^\circ\text{C}$ is the loss of the trimesic acid ligand as the material begins to decompose.

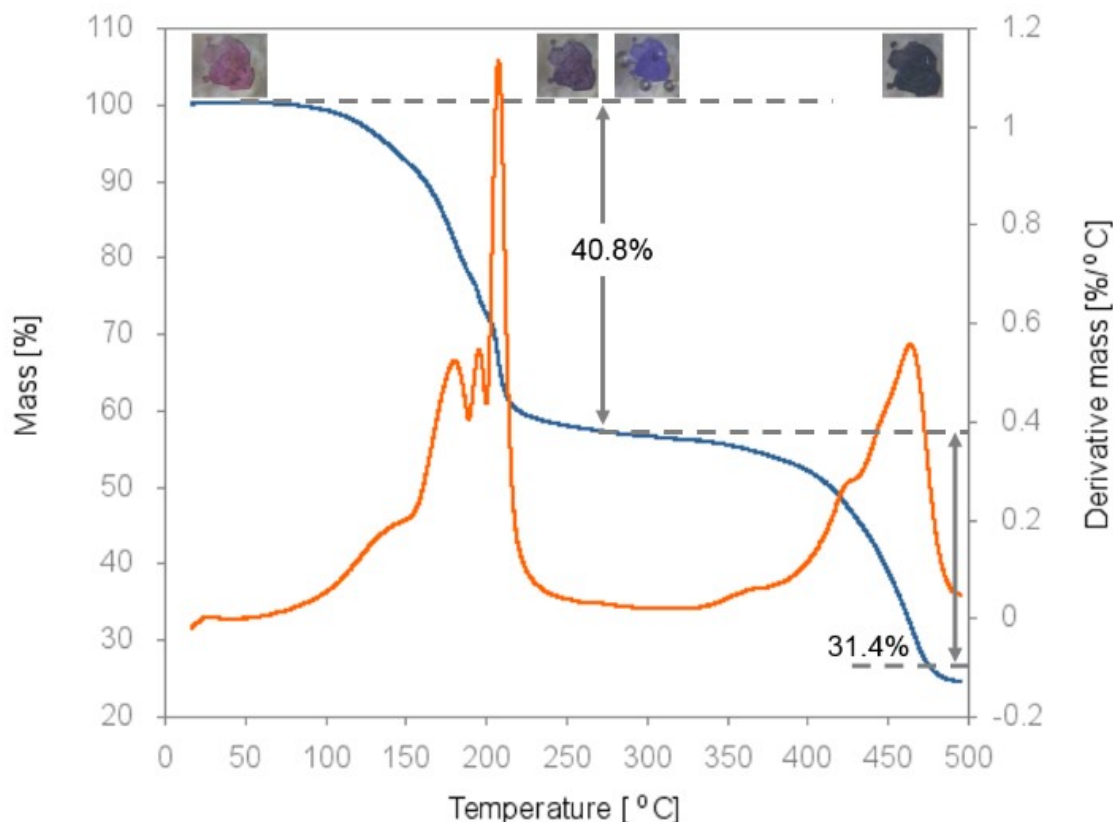


Fig. S6. Overlay of TGA and first derivative plots of **1**. This shows a three-step mass loss (40.8%) of the uncoordinated and coordinated DMF.

The pink crystals darken upon heating and are purple by $200\text{ }^\circ\text{C}$ as solvent is lost (Fig. S7). This colour change may be attributed to a change in the geometry of the Co(III) metal centre from octahedral to tetrahedral as the axial coordinated DMF are removed. Bubbling starts at $200\text{ }^\circ\text{C}$ and the crystal turn opaque once bubbling has stopped. The material continues to darken and is dark blue at $400\text{ }^\circ\text{C}$. The overall shape of the crystals is maintained; however, hairline cracks are seen as the material is heated.

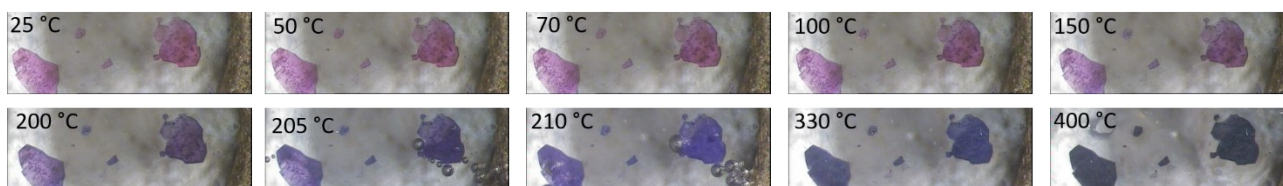


Fig. S7: Hot stage images of **1**. The crystals darken from pink to purple upon heating. All DMF has been removed by $220\text{ }^\circ\text{C}$.

Solvent exposure

Table S4. Table of relative polarities of solvents used.

Solvent	Relative polarity
MeCN	0.460
PhCN	0.333
EtOH	0.654
Ether	0.117
MeOH	0.762
Water	1.000

Fig. S8 and Fig. S9 show the TGA and PXRD results after immersing **1** in various solvents for 24 h and room temperature.

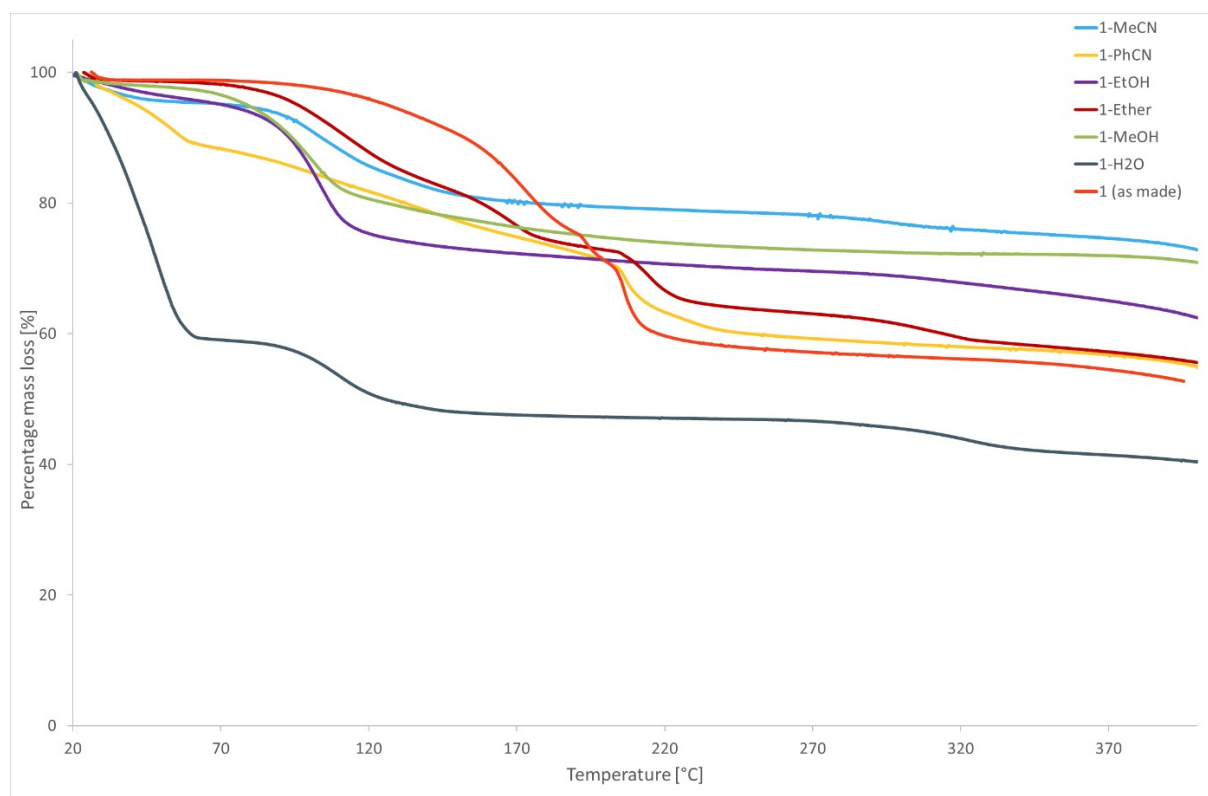


Fig. S8. TGA plots after soaking of crystals of **1** in various solvents for 24 h resulting in **1**-solvent.

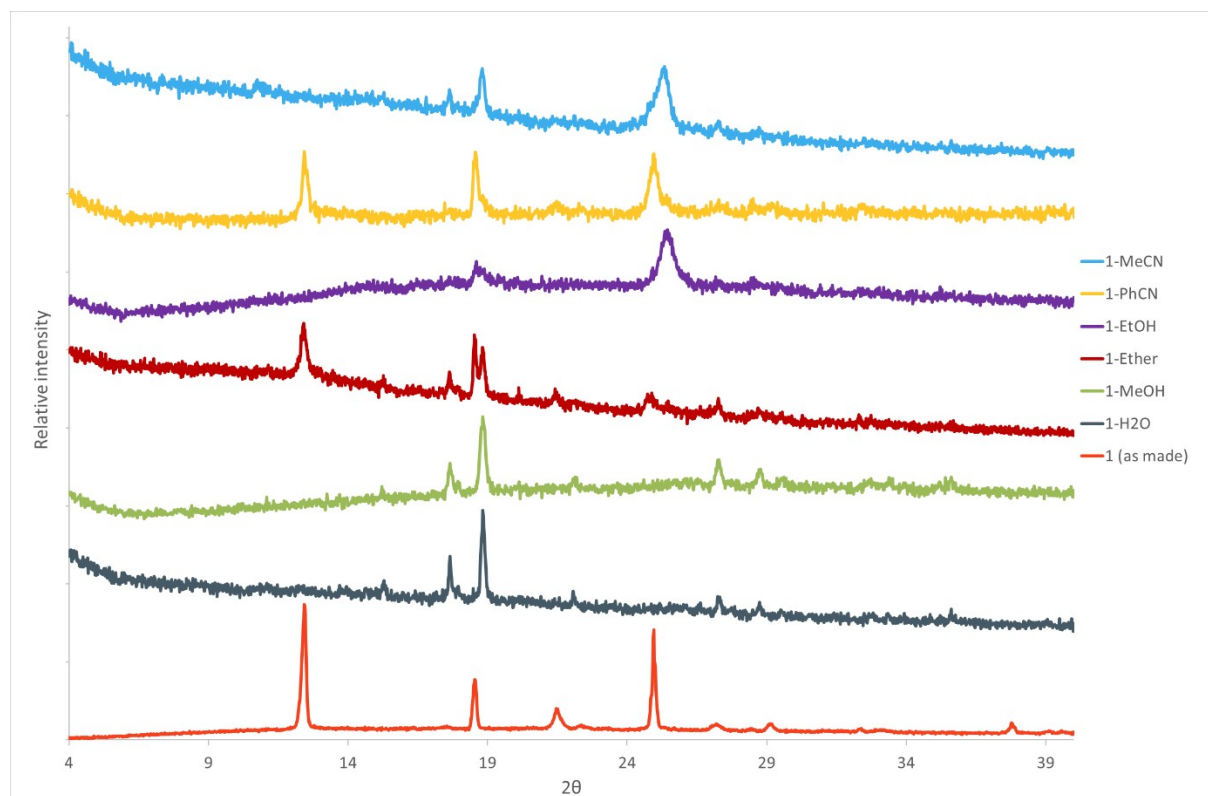


Fig. S9. PXRD patterns after the crystals of **1** have been immersed in different solvents for 24 h. Changes are attributed to different solvents in the crystal structure.

Reversibility

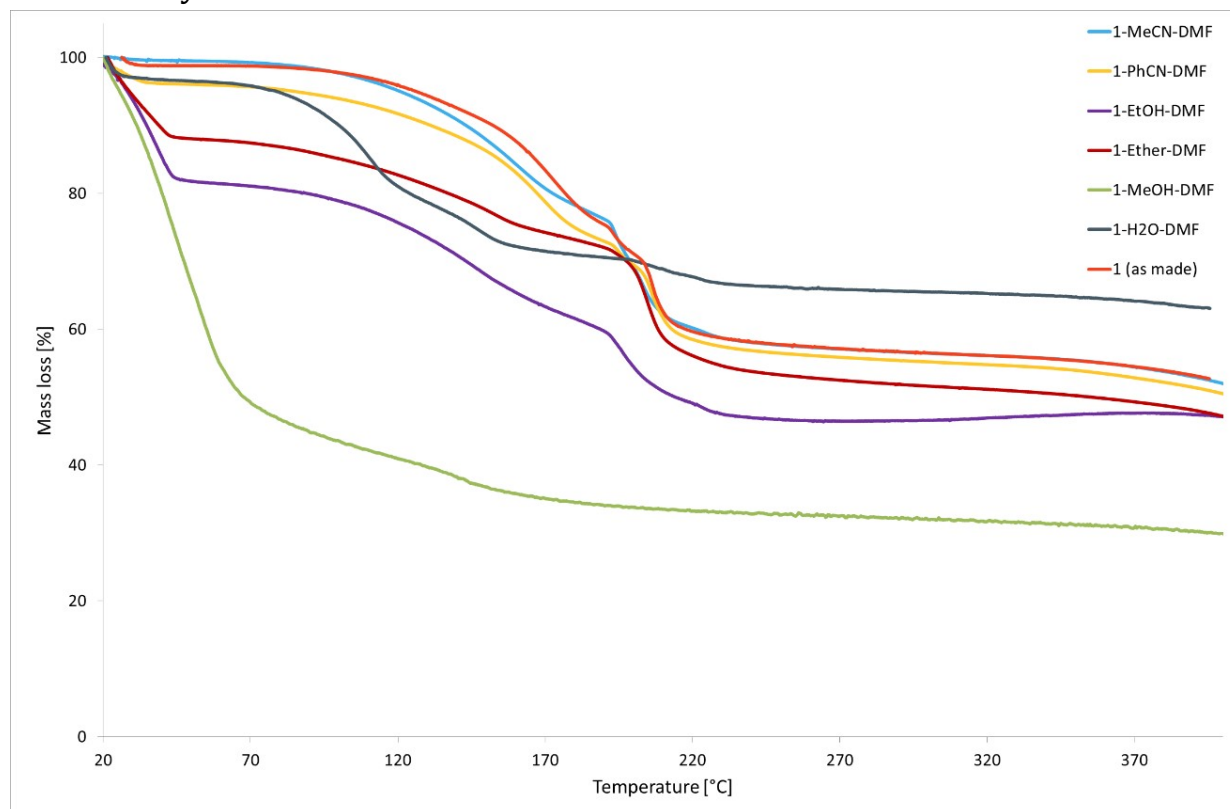


Fig. S10. Reversibility of solvent exchange. TGA solvent exchange, after exposure of 1-solvent is immersed in DMF, resulting in 1-solvent-DMF

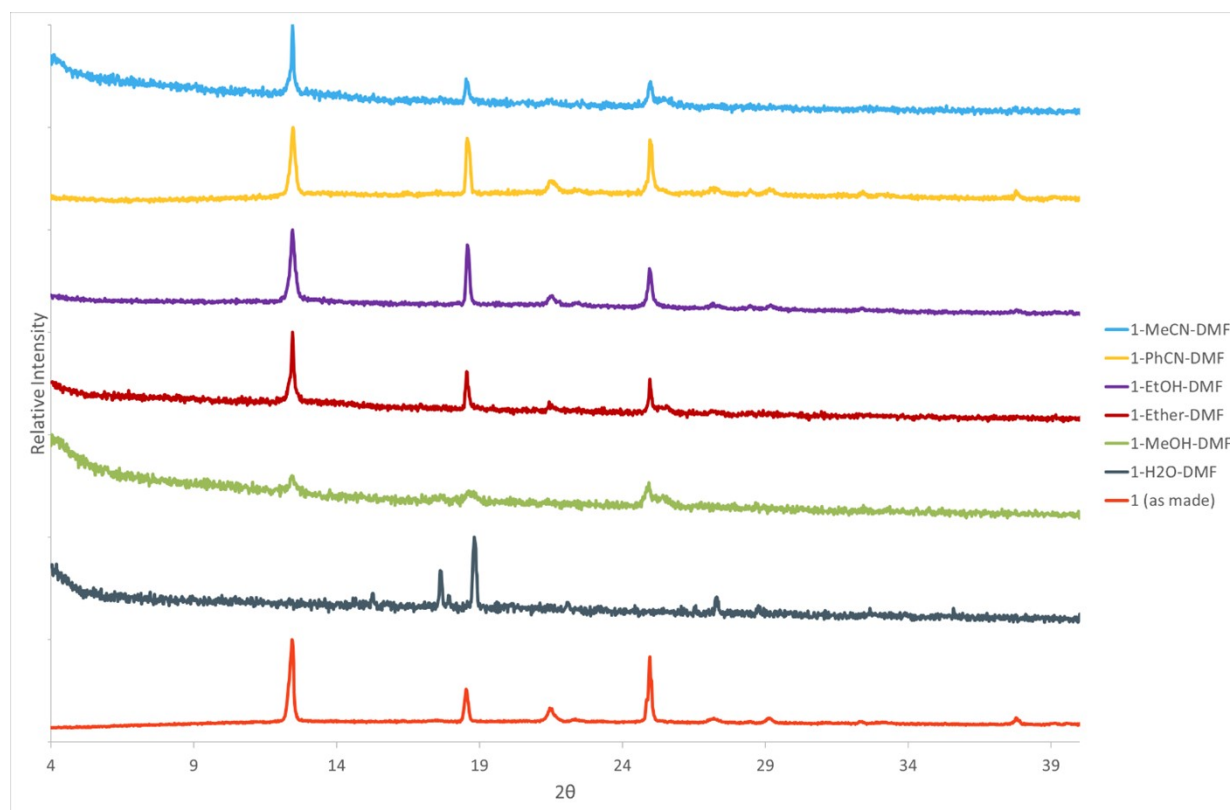


Fig. S11. Reversibility of solvent exchange. PXRD patterns of 1-solvent after immersed in DMF, resulting in 1-solvent-DMF

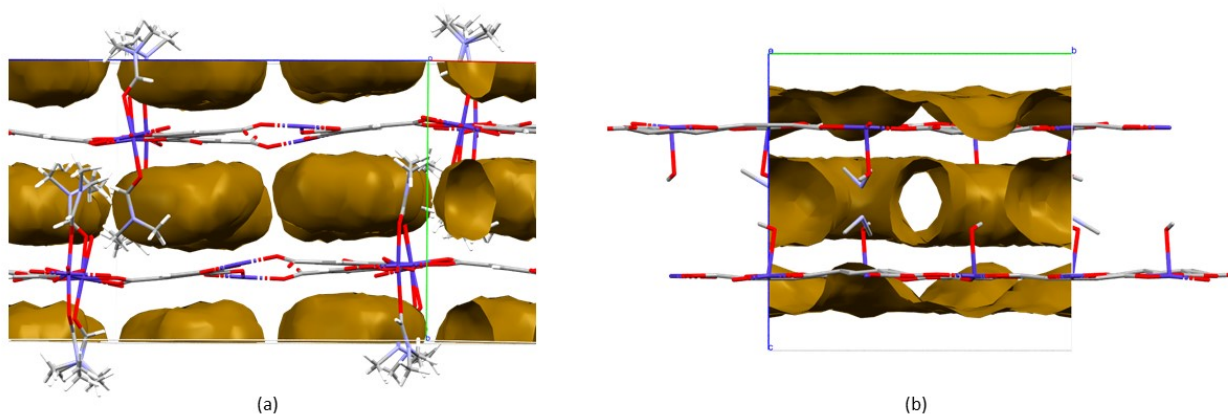


Fig. S12. Analysis of voids in (a) **1** and (b) **2**, carried out using Mercury with probe radius 1.2 Å with approximate grid spacing of 0.7 Å. For **1**, the contact surface area is 1635 Å³ (24.1% of unit cell volume), while for **2** it is 1706 Å³ (50.7% of unit cell volume)

Exposure of **1** to acetonitrile (MeCN)



Fig. S13. Crystals after soaking **1** in MeCN for 24 h.

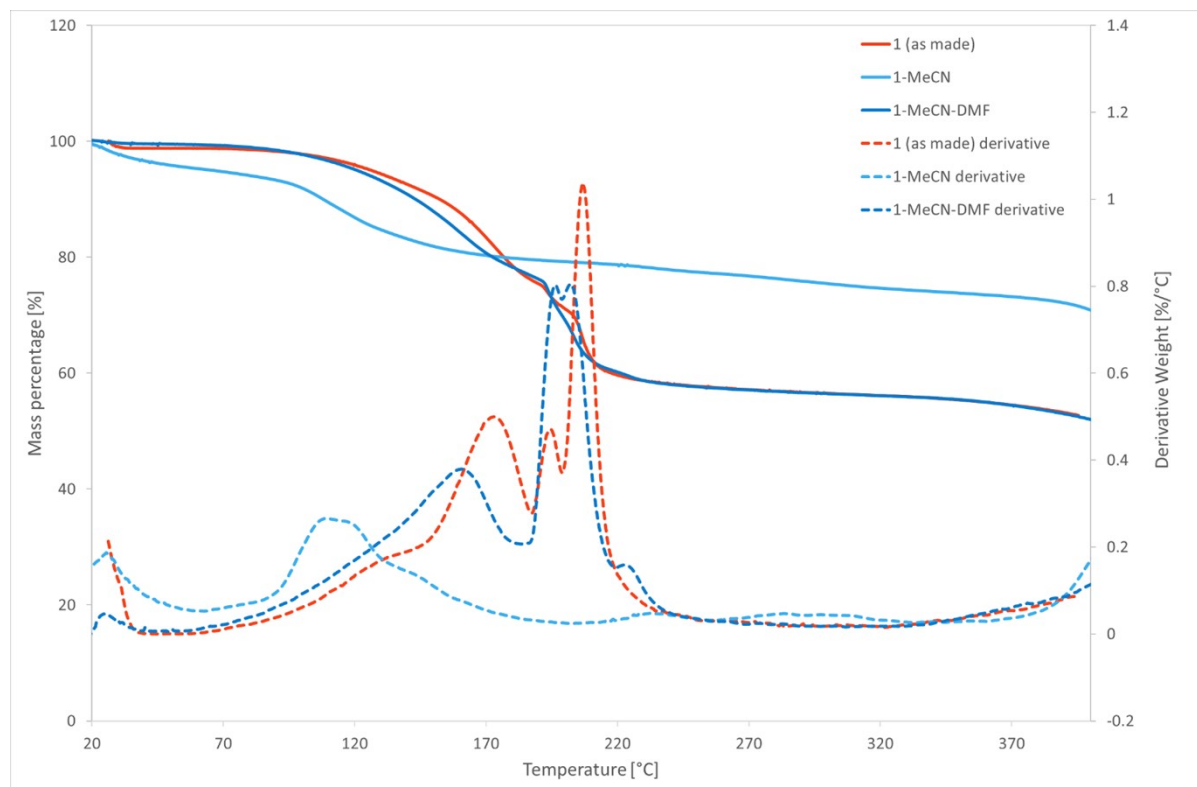


Fig. S14. TGA traces for MeCN experiments: **1** is soaked in MeCN resulting in **1-MeCN**, then soaked in DMF resulting in **1-MeCN-DMF**.

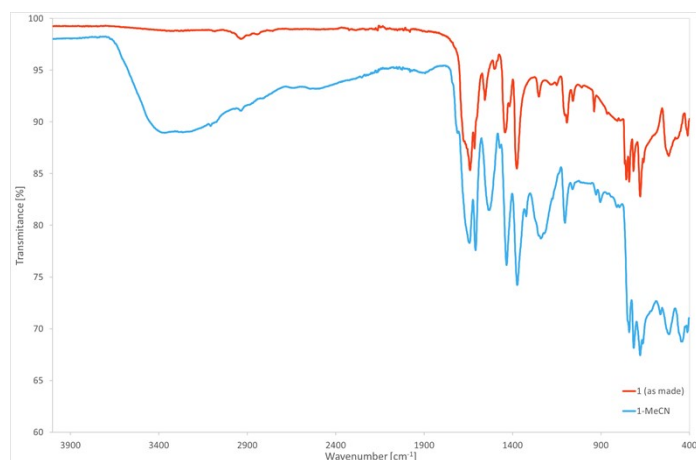


Fig. S15. Comparison of FT-IR spectra of **1** before (orange) and after (light blue) immersion in MeCN resulting in **1-MeCN**.

Exposure of **1** to benzonitrile (PhCN)

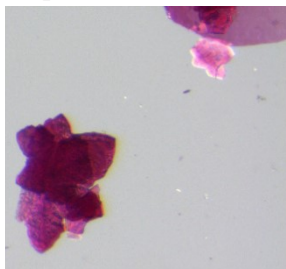


Fig. S16. Crystals after immersing **1** in PhCN for 24 h resulting in **1-PhCN**

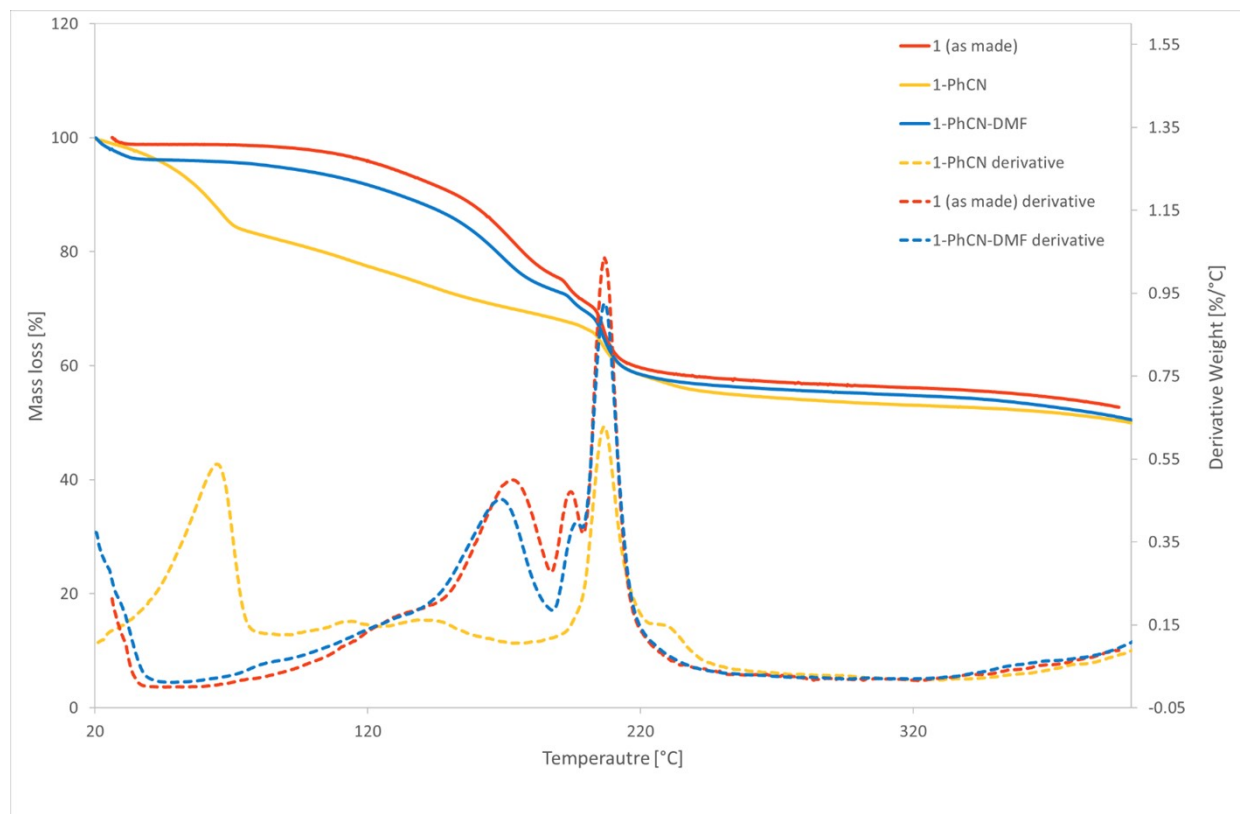


Fig. S17. TGA traces of PhCN experiments: **1** is soaked in PhCN resulting in **1-PhCN**, then soaked in DMF resulting in **1-PhCN-DMF**.

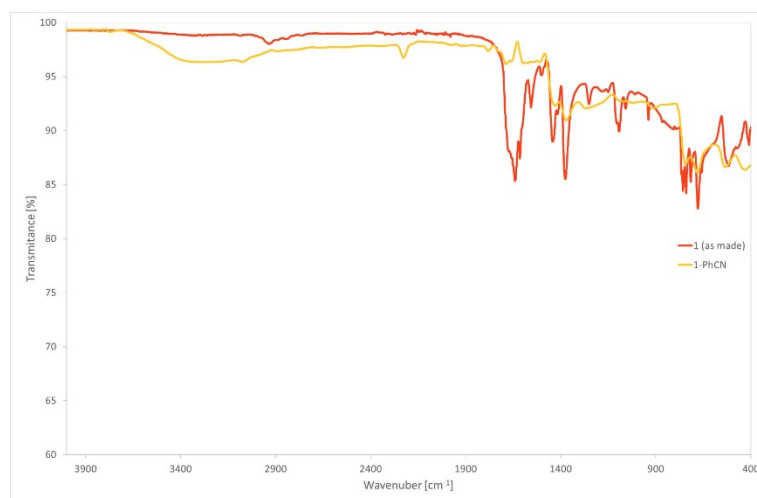


Fig. S18. Comparison of FT-IR spectra after immersing **1** in PhCN resulting in **1-PhCN** (or **2**).

Exposure of **1** to Ethanol (EtOH)

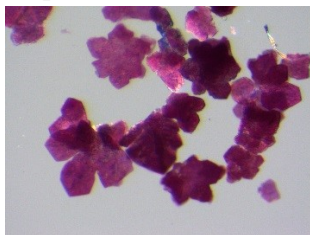


Fig. S19. Crystals of **1** after soaking in EtOH for 24 h.

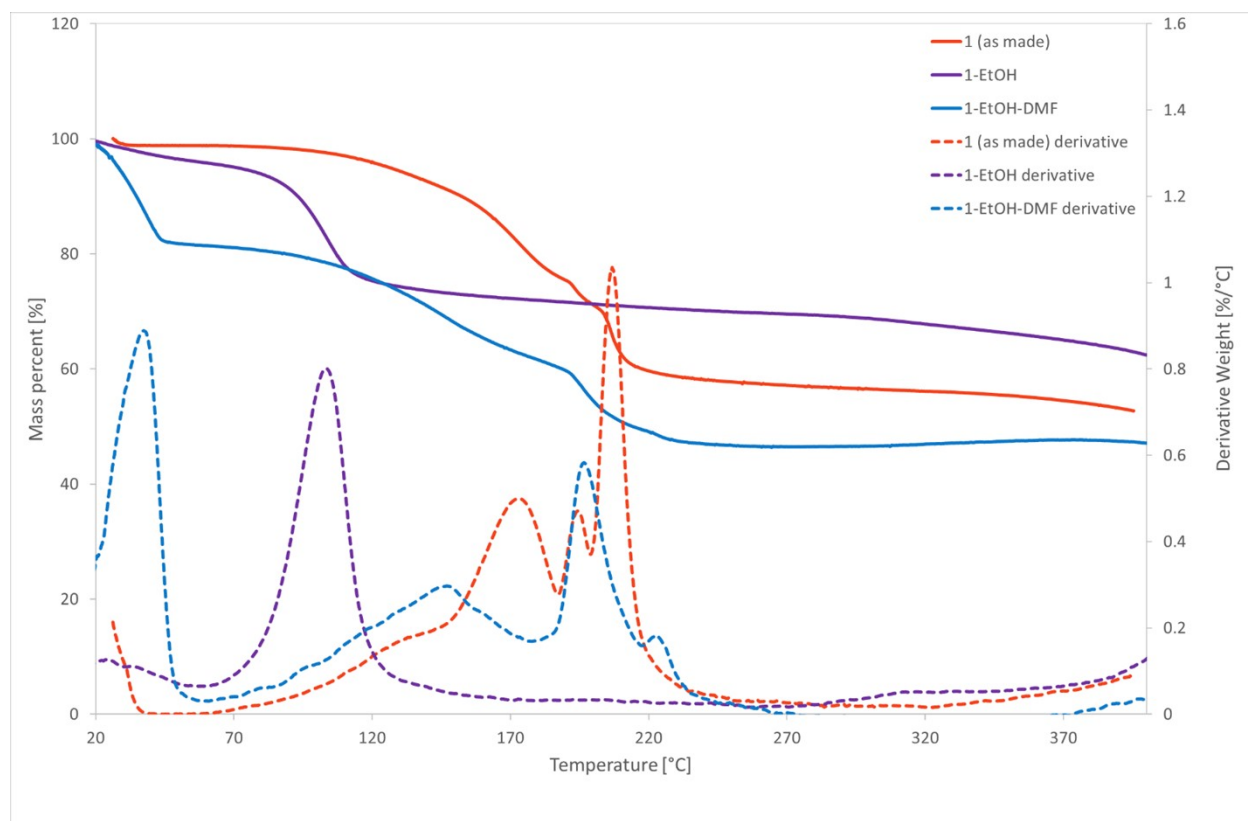


Fig.S20. TGA traces of EtOH experiments: **1** is immersed in EtOH resulting in **1-EtOH**, then soaked in DMF resulting in **1-EtOH-DMF**.

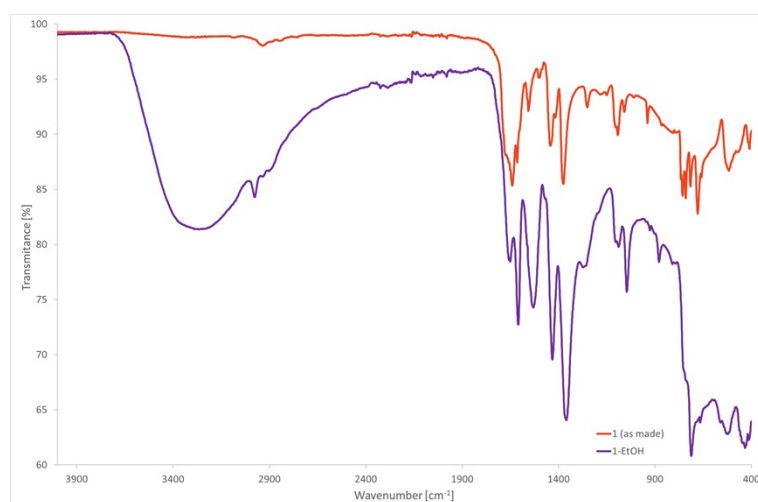


Fig. S21. Comparison of FT-IR patterns of **1**, before (orange) and after (purple) soaking in EtOH for 24 h, resulting in **1-EtOH**.

Exposure of **1** to Diethyl ether



Fig. S22. Crystal of **1** after immersed in diethyl ether (**1-Ether**).

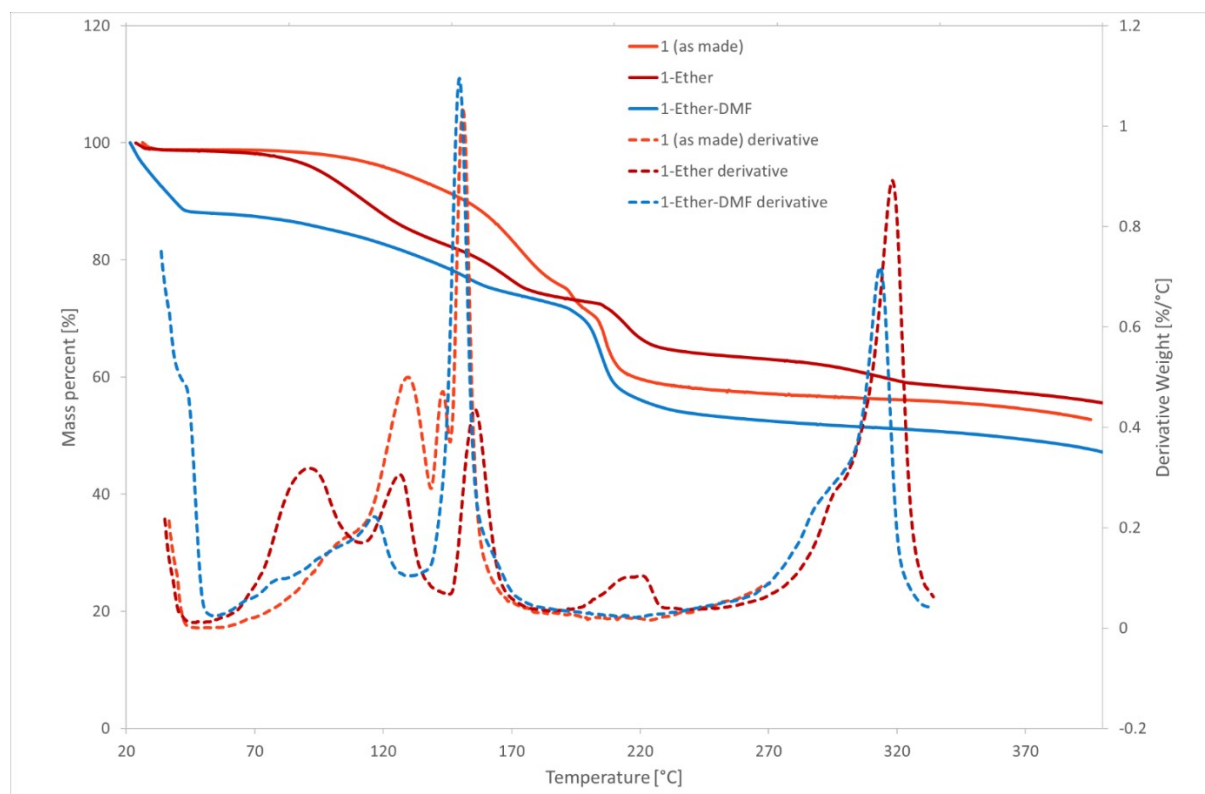


Fig. S23. TGA traces for **1** after ether experiments: **1** is soaked in Ether resulting in **1-Ether**, then soaked in DMF resulting in **1-Ether-DMF**.

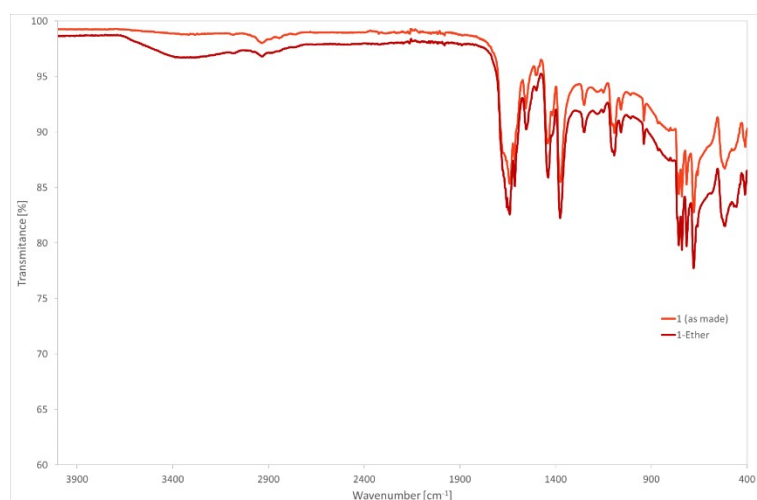


Fig. S24. Comparison of FT-IR spectra after (orange) soaking of **1** (red) in ether resulting in **1-Ether**

Exposure of **1** to methanol (MeOH)

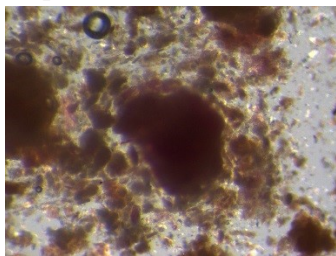


Fig. S25. Pale pink crystal of **1** after immersion in MeOH for 24 h (**1**-MeOH).

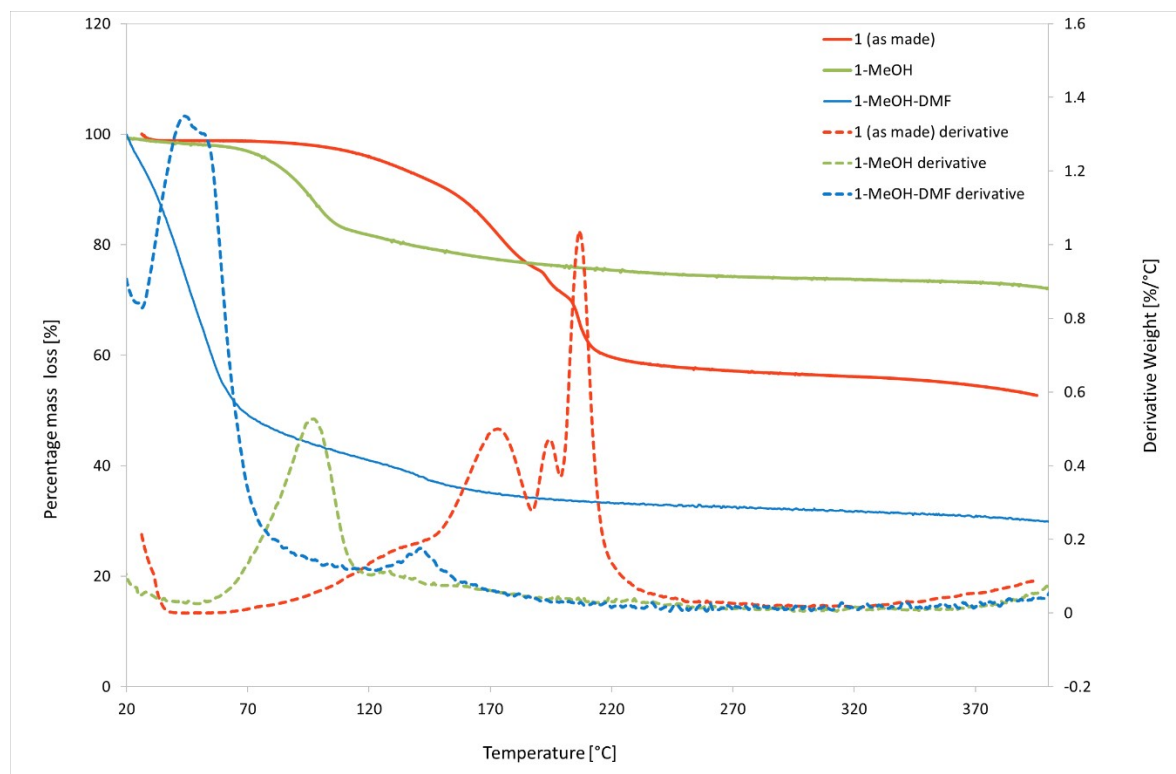


Fig. S26. TGA traces for **1** after MeOH experiments: **1** is immersed in Ether resulting in **1**-MeOH, then soaked in DMF resulting in **1**-MeOH-DMF.

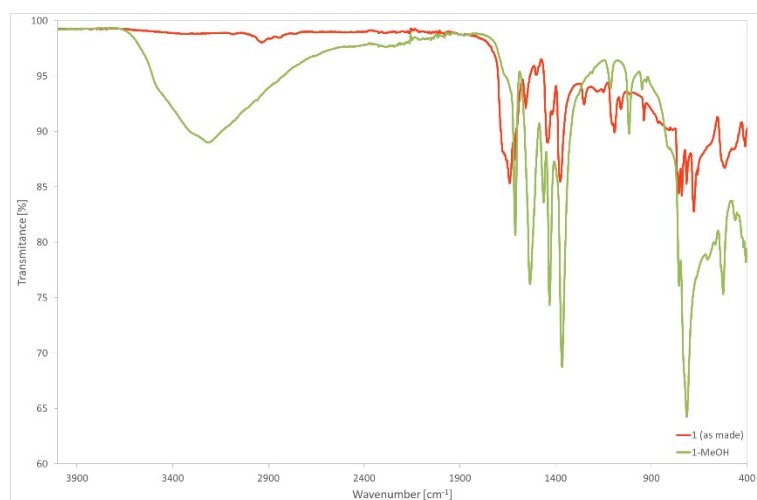


Fig. S27. Comparison of FT-IR spectra after (green) soaking of **1** (red) in ether resulting in **1**-MeOH.

Exposure of **1** to Water

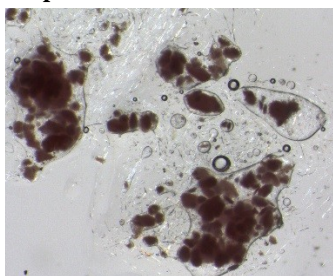


Fig. S28. Crystals of **1** after 24 h water exposure – crystals appear degraded.

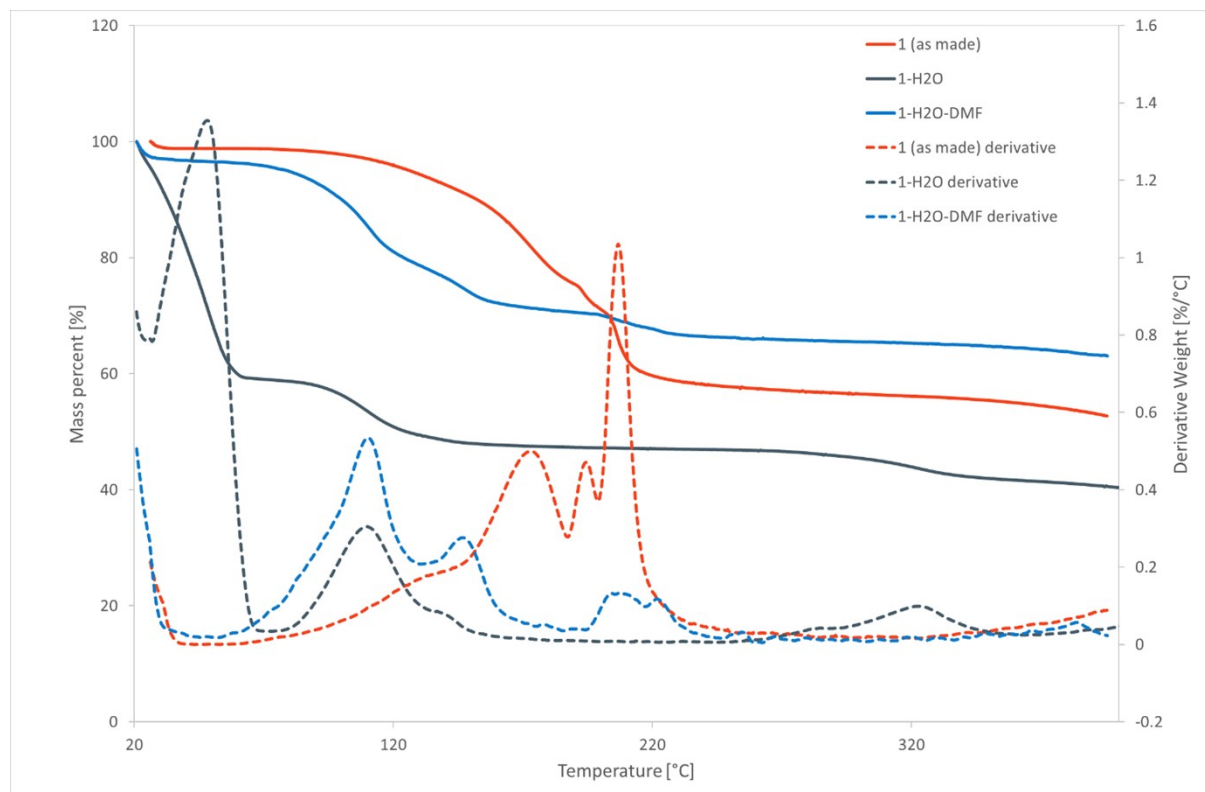


Fig. S29. TGA traces for **1** after ether experiments: **1** is soaked in water resulting in **1-H2O**, then soaked in DMF resulting in **1-H2O-DMF**.

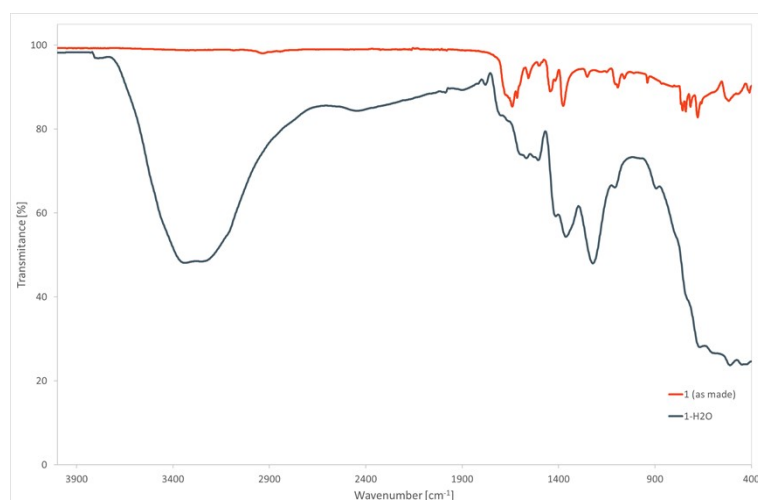


Fig. S30. Comparison of FT-IR spectra of **1** before (orange) and after (grey) soaking in water resulting in **1-H2O**.

Sorption by framework of **1** (**1-f**)

To remove the guest DMF from **1**, **1** was dried in a vacuum oven, at 85 °C for 24 h. The purple material can be seen in Fig. S30. This guest free material was immersed various solvents. Only MeOH and water were sorbed (Fig. S31 and Fig. S32).



Fig. S31. Left: material after drying in a vacuum oven for 24 h at 85 °C (**1-f**), the guest DMF has been removed. Right: blue crystals of **1** post TGA. The crystals after heating during TGA to 400 °C.

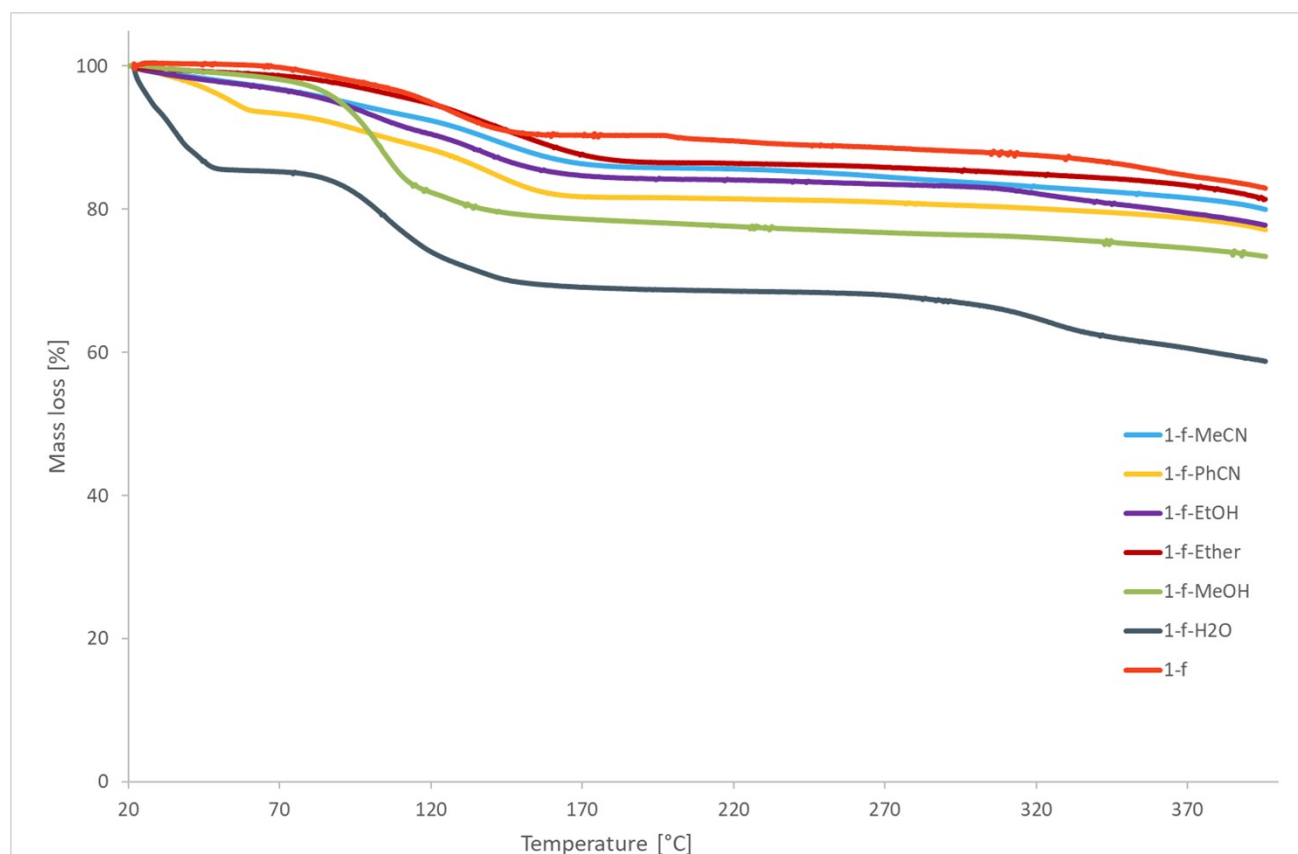


Fig. S32. TGA traces after immersion of **1-f** in various solvents for 24 h. Only MeOH and water are sorbed.

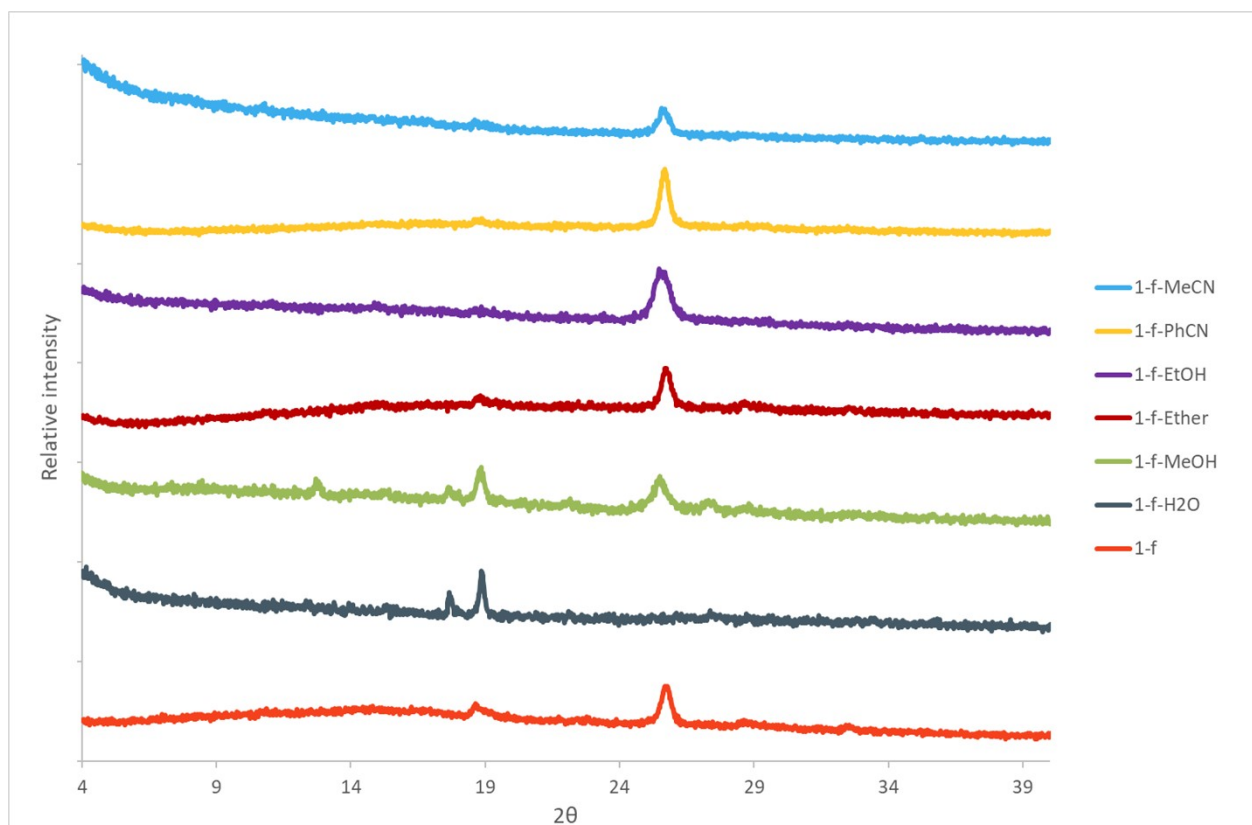


Fig. S33. PXRD patterns after **1-f** is immersed for 24 h in various solvents resulting in **1-f-solvent**. Crystallinity is greatly reduced during the drying process.

The following DSC traces show the result of immersing **1-f** in various solvents (Fig S34, Fig. S35, Fig. S36, Fig. S37, Fig. S38, Fig S39).

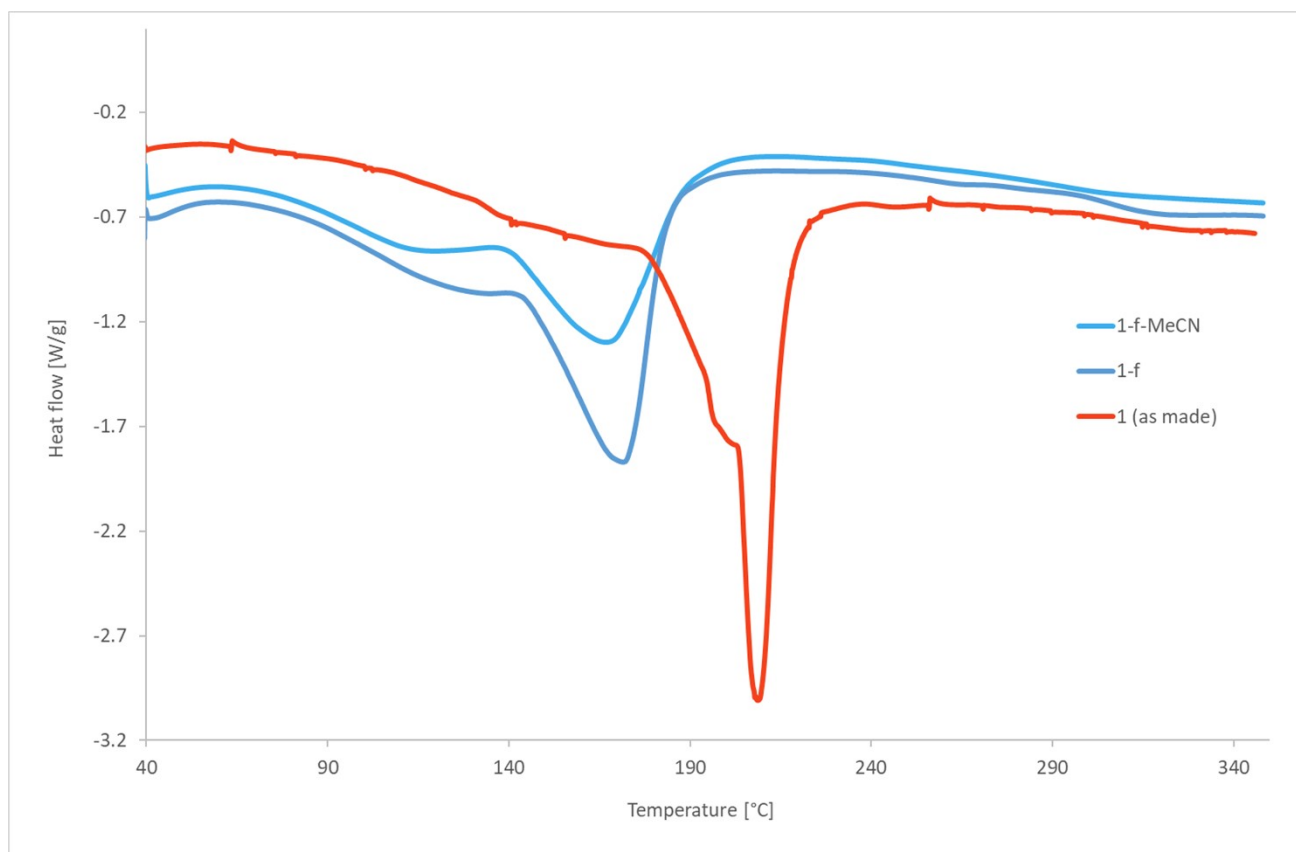


Fig. S34. DSC trace of **1**, **1-f** and **1-f-MeCN** after immersing **1-f** in MeCN for 24 h. MeCN is not taken up by **1-f**.

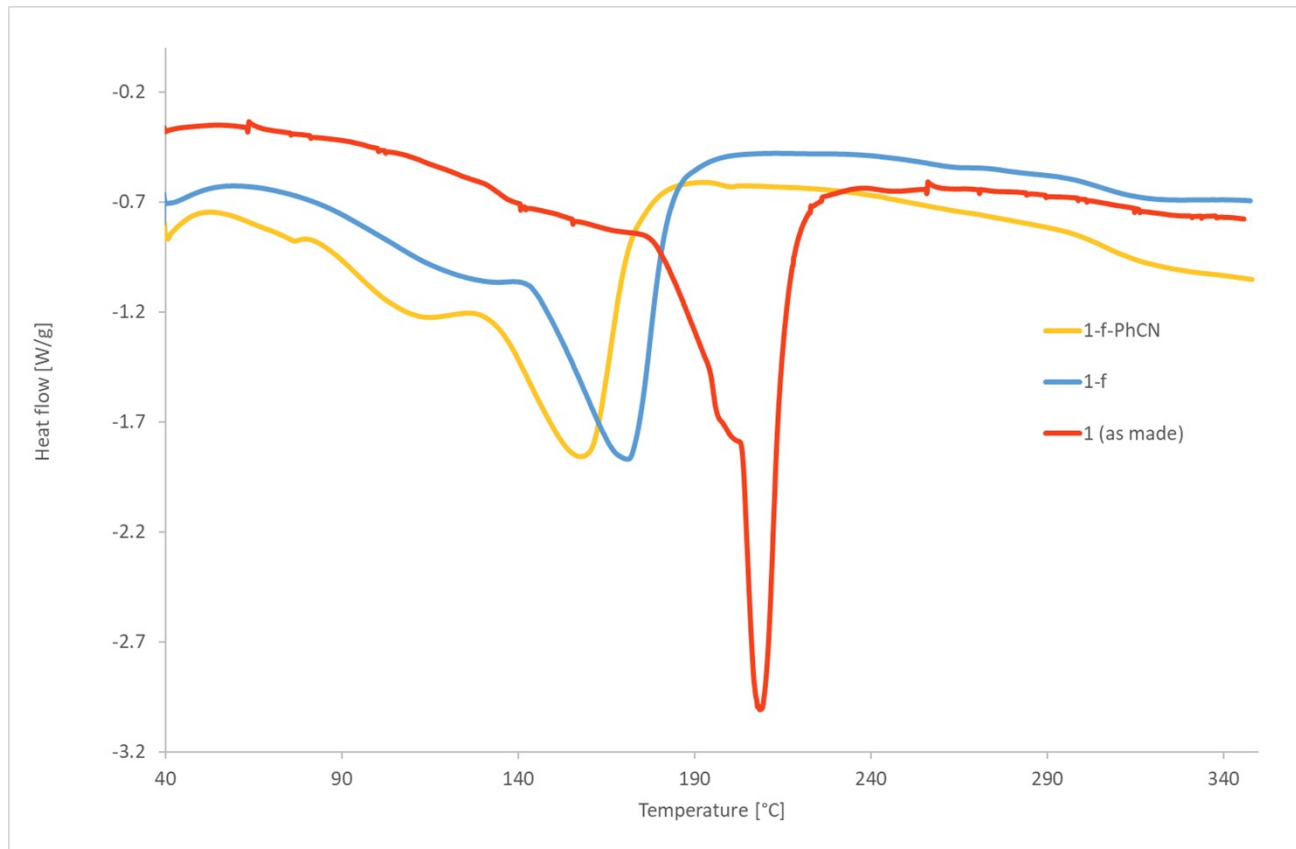


Fig. S35. DSC trace of **1**, **1-f** and **1-f** after immersion in PhCN for 24 h. PhCN is not taken up by **1-f**.

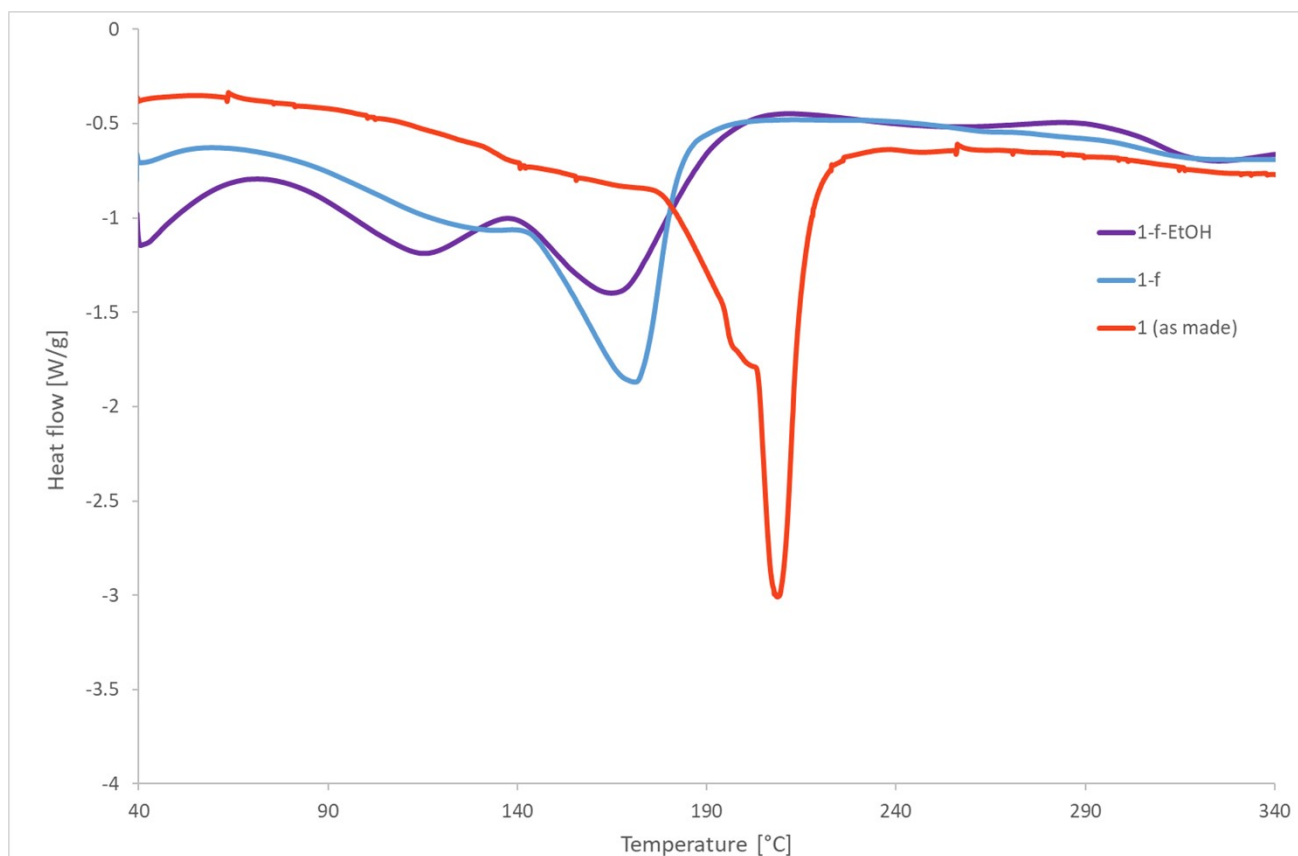


Fig. S36. DSC trace of **1**, **1-f** and **1-f** after immersion in EtOH for 24 h (**1-f-EtOH**). Ethanol is not taken up by **1-f**.

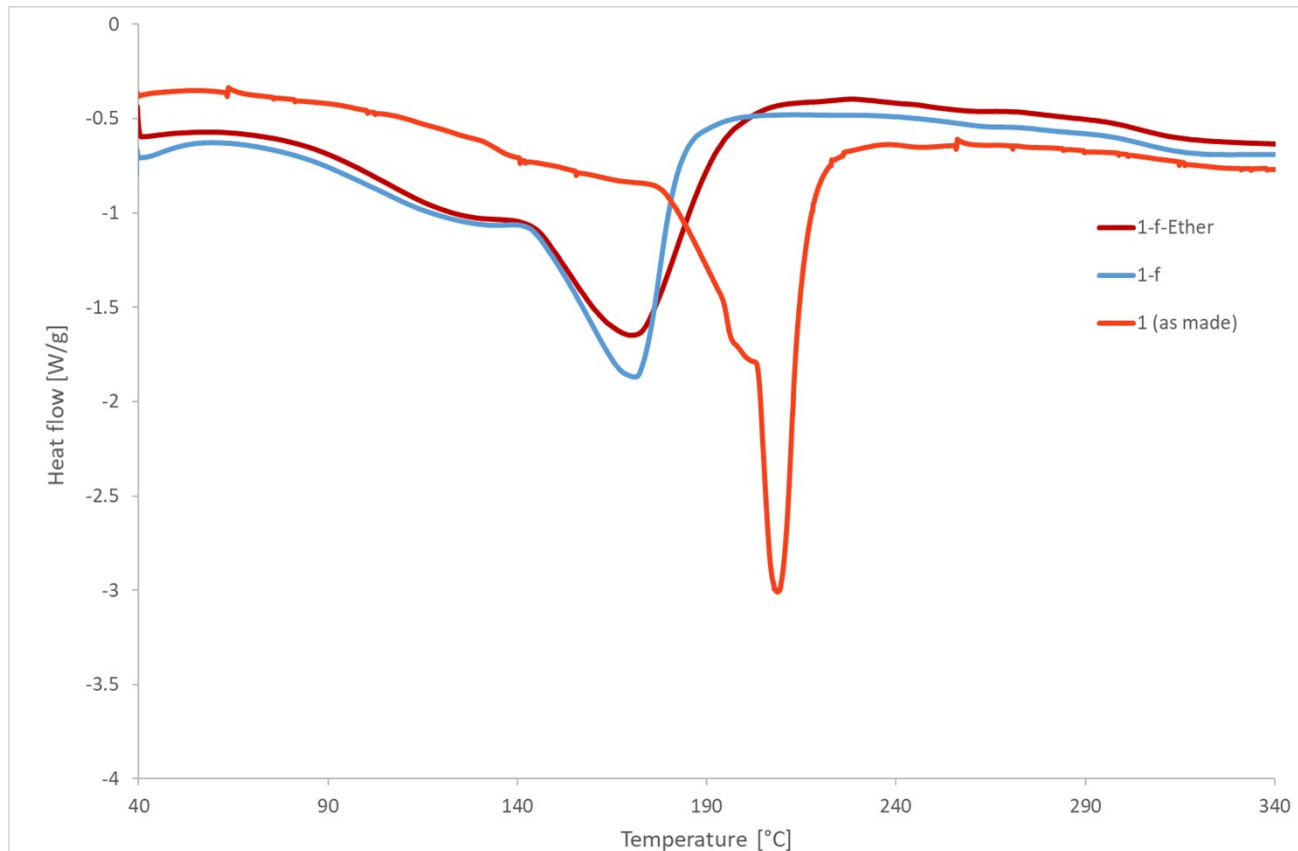


Fig. S37. DSC trace of **1**, **1-f** and **1-f** after exposure soaking in Ether for 24 h (**1-f-Ether**). Ether is not sorbed by **1-f**.

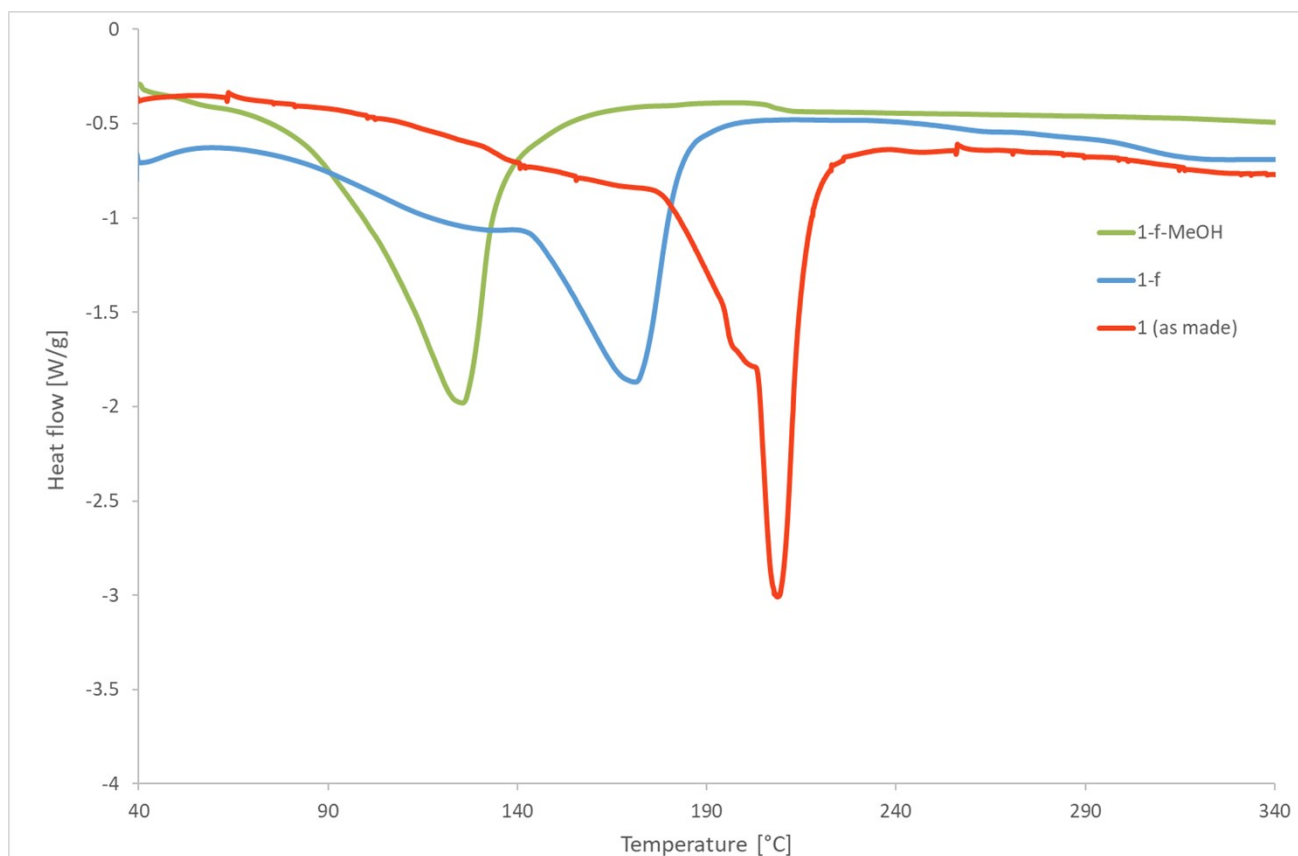


Fig. S38. DSC trace of **1**, **1-f** and **1-f** after immersion in MeOH for 24 h. MeOH is sorbed by **1-f**.

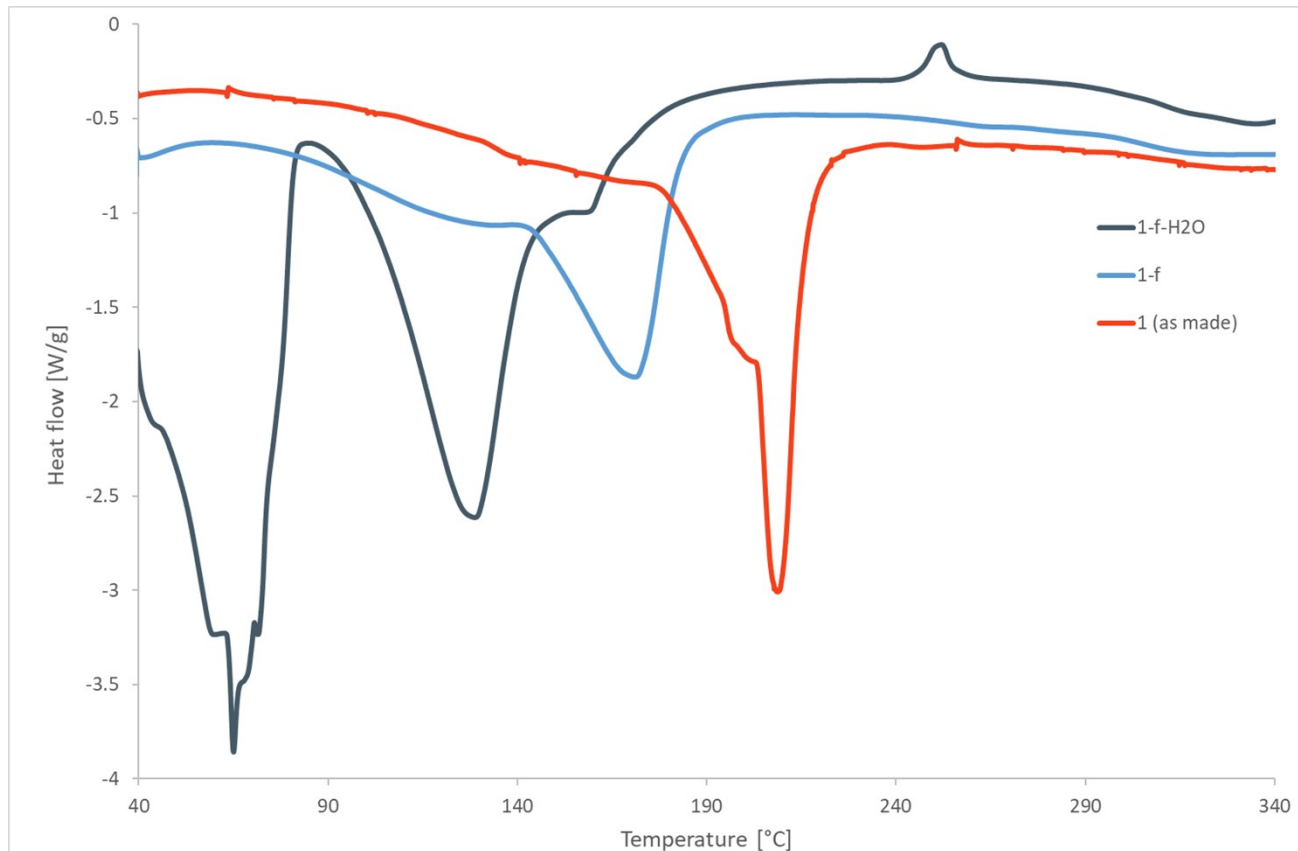


Fig. S39. DSC trace of **1**, **1-f** and **1-f** after immersion in water for 24 h. H₂O is sorbed by **1-f**.